Perpetual bioplastic production by a cyanobacteria-dominated microbiome

Beatriz Altamira-Algarra[1], Artai Lage[1], Ana Lucía Meléndez[1], Marc Arnau[2,3], Eva Gonzalez-Flo[1], Joan García[4]

[1] GEMMA-Group of Environmental Engineering and Microbiology. Department of Civil and Environmental Engineering. Escola d'Enginyeria de Barcelona Est (EEBE). Universitat Politècnica de Catalunya-BarcelonaTech. Av. Eduard Maristany 16. Building C5.1. E-08019 Barcelona. Spain

[2] IMEM-Innovation in Materials and Molecular Engineering. Departament d'Enginyeria Química, EEBE, Universitat Politècnica de Catalunya, C/Eduard Maristany 10-14, Barcelona, Spain

[3] Barcelona Research Center in Multiscale Science and Engineering, EEBE, Universitat Politècnica de Catalunya, C/Eduard Maristany 10-14, Barcelona, Spain

[4] GEMMA-Group of Environmental Engineering and Microbiology. Department of Civil and Environmental Engineering. Universitat Politècnica de Catalunya-BarcelonaTech. c/ Jordi Girona 1-3. Building D1. E-08034 Barcelona. Spain

* Corresponding author: joan.garcia@upc.edu

Abstract

Departing from the conventional axenic and heterotrophic cultures, our research ventures into unexplored territory by investigating the potential of photosynthetic microbiomes for polyhydroxybutyrate (PHB) production. A cyanobacteria-rich microbiome was harnessed for PHB production in a 3 L photobioreactor under non-sterile conditions. The robust culture achieved up to 28 $\%_{dcw}$ PHB over 108 days of alternating growth and accumulation phases. Nile Blue staining and Transmission Electron Microscope visualization successfully confirmed the presence of PHB granules within cyanobacteria cells. Analysis through proton Nuclear Magnetic Resonance further validated the extracted polymer as PHB. In addition, the overexpression of the enzyme PHA synthase throughout the accumulation phase correlated directly with the increased PHB production. Also, gene expression changes suggested that initially, glycogen served as the primary storage compound. However, with prolonged macronutrient stress, there was a shift of the carbon flux towards favoring PHB synthesis. Overall, it was demonstrated for the first time the feasibility of using a phototrophic microbiome to continuous production of PHB in a non-sterile system, contributing to advancing in the field of biopolymer production and offering valuable insights into the metabolic pathways involved.

Introduction

Environmental biotechnologies involving cyanobacteria for bioproduct generation still today face enormous scientific challenges. While numerous research have repeatedly highlighted cyanobacteria's exceptional potential for bioproducts[1–3], full-scale applications beyond the food industry remain limited. Bridging research gaps related to cyanobacterial cultures and their culture conditions is crucial to unlocking their full potential.

Among the several bioproducts synthetized by cyanobacteria, polyhydroxyalkanoates (PHA) stand out as particularly intriguing as a source for environmentally friendly non-petrochemical-based plastics[4]. Cyanobacteria can accumulate polyhydroxybutyrate (PHB, a type of PHA) under nutrient-limited conditions[2,5–8]. Nevertheless, the productivity achieved up to now by cyanobacteria wild-type (wt) strains monocultures in autotrophic conditions is not very high, being usually lower than 15 % dry cell weight (dcw) PHB. In some cases, remarkably high values of up to 20-25 $\%_{dcw}$ PHB have been reported in wild-type (wt) strains[6,9]. To enhance productivity, molecular biology techniques as introducing, overexpressing or deleting genes involved in PHB metabolism have been used[10]. However, to make PHB production processes a reality in an industrial context and cost-competitive with the current plastic market, the use of engineered strains seems not to be the most suitable strategy. An alternative procedure involves supplementing cultures with an external organic carbon source, like acetate (Ac). This has led to PHB production of up to 46 $\%_{dcw}$ PHB by cyanobacteria monocultures of *Anabaena* sp.[11], 26 $\%_{dcw}$ PHB by *Synechoccocus* sp.[6] and 22 $\%_{dcw}$ PHB by *Synechocystis* sp.[12]

Nevertheless, monocultures require precise control and sterile conditions, driving up production costs. An option could be the use of microbiomes (or mixed cultures), which in principle could have more stability than single strain cultures when growing in complex media. Microbiomes are potentially more resilient to fluctuations in environmental conditions and less susceptible to contamination with competing microorganisms. Probably, the most well-known microbiome for environmental applications is activated sludge. Studies with these organisms under heterotrophic conditions report up to 60 $\%_{dcw}$ PHB[13,14]. Nevertheless, to the authors' knowledge, the use of photosynthetic microbiomes enriched with cyanobacteria for PHB production has only been tested in very few studies, including[5,15–17].

A crucial research gap that needs to be addressed in cyanobacterial biotechnology is how to maintain productive cultures for the long-term bioproducts generation. Unfortunately, most experiments to date have been limited to short time, typically lasting only a few weeks and small-scale batch experiments under sterile conditions[8,10,18]. There have been no attempts to maintain cultures in the long term (at least for several months) for continuous bioproduct generation.

In a previous study, we assessed the viability of augmenting PHB production by enhancing the population of biopolymer-producing organisms via a dual-phase approach involving alternating cell growth on PHB and subsequent biopolymer accumulation induced by Ac addition in a dark environment[17]. Although up to 22 $\%_{dcw}$ PHB was obtained after 179 days of operation, the presence of competing green algae resulted in the destabilization of the microbiome and ultimately led to the green algae outcompeting the biopolymer-producing organisms, thus hampering PHB production stability.

In light of the above, in the present study we demonstrated for the first time the capacity of a photosynthetic microbiome enriched in cyanobacteria (and without green algae) to produce PHB over a sufficient extended period to prove perpetual production. To achieve this, we cultivated a microbiome in a photobioreactor for a total of 129 days, alternating growth/accumulation phases in controlled but non-sterile conditions. Nile Blue A staining and Transmission Electron Microscopy (TEM) were used to visualize intracellular PHB granules. We also analyzed gene expression by quantitative real-time PCR (RT-qPCR) to explore the metabolic pathways involved in PHB synthesis. Finally, the extracted polymer characterization was performed by means of Raman Spectroscopy, Fourier Transform Infrared Spectroscopy (FTIR) and proton Nuclear Magnetic Resonance (^{1}H-NMR).

The results of this study shed light on the long-term capabilities of cyanobacterial microbiomes to generate PHB, which could have significant implications for the bioplastics industry.

Results

Consistent growth and PHB accumulation by microbiome R3

We started the study by inoculating two photobioreactors (PBRs) with 100 mg volatile suspended solids (VSS)·L^{-1} of microbiome R3 obtained in[16]. The study began with the

growth phase of the conditioning cycle (Supplementary Fig. 1). A steady-state was reached at the fourth day, when the biomass (as VSS) was approximately 800 mgVSS·L^{-1} (Fig. 1). The average specific growth rate was 0.52 d^{-1} (Table 1), higher than that obtained with monocultures of *Synechocystis* sp. under similar culture conditions[6,19]. However, it took 18 days for N to be completely depleted (Supplementary Fig. 2); likely due to P limitation since it was maintained at a relatively low value (0.1 mgP·L^{-1}) to favour cyanobacteria and avoid green microalgae growth. At this point, the accumulation phase started by adding 600 mgAc·L^{-1} to the medium and enclosing the PBRs with opaque PVC tubes. Starvation phase was maintained 14 days to follow the time course of PHB synthesis by this microbiome. Biomass concentration remained constant during this phase (Fig. 1). Interestingly, biomass synthetized 11 $\%_{dcw}$ PHB during the growth phase, although the conditions were not ideal for biopolymer accumulation due to nutrient presence. Nevertheless, previous studies[18] have reported significant PHB synthase activity, the enzyme involved in biopolymer synthesis, in growing cells of *Synechocystis* sp. PCC6803, the same cyanobacteria strain identified in the microbiome under investigation[16].

Biopolymer accumulation increased from 11 $\%_{dcw}$ to 27 $\%_{dcw}$ in seven days, when it reached the maximum. After that, PHB production slowly decreased, since at day 14 (end of the accumulation phase) PHB content was 21 $\%_{dcw}$ (Fig. 1). During this period, biomass consumed 470 mgAc·L^{-1} from the 600 mgAc·L^{-1} added (Supplementary Fig. 2).

After 14 days in accumulation phase, a biomass purge was done and replaced with fresh BG-11 medium to start a new cycle (repetition 1) (Supplementary Fig. 1). Subsequent growth phases (repetition 1, 2 and 3) aimed to select PHB-producers because we assumed that the cyanobacteria will use mostly the stored PHB as carbon source since no substrate (as carbon source) was added to the medium (only the CO_2 from the injections to maintain pH, Supplementary Fig. 3).

To shorten the growth phase, we used a lower N concentration (25 mg·L^{-1}) during the repetitions' growth phase. This adjustment did not hinder the biomass growth. In fact, biomass reached an average of almost 800 mgVSS·L^{-1} in seven days (Fig. 1 and Supplementary Fig. 2), sufficient for the accumulation step[17]. Biomass exhibited an average growth rate of 0.17 d^{-1} (Table 1) in repetitions 1-3, three times slower than in the first growth performed in the conditioning cycle (μ = 0.52 d^{-1}). This difference can be attributed to a lower initial biomass concentration (100 mgVSS·L^{-1} vs. 400 mgVSS·L^{-1}),

121 combined with the presence of external IC (as bicarbonate), as well as higher N
122 concentration (50 $mg \cdot L^{-1}$ vs 25 $mg \cdot L^{-1}$) in the conditioning cycle. PHB concentration
123 declined from the beginning to the end of each growth phase, indicating that cells used
124 the stored PHB as carbon source. Growth rate on PHB seems to be slower than that on
125 soluble IC because growth rate on biopolymer is determined by the PHB hydrolysis rate,
126 which is a slow process[17,20].

127 Regarding to PHB production, both PBRs followed a similar trend (Fig. 1). Intracellular
128 PHB increased after Ac supplementation and 14 days in dark, peaking at day 4 of the
129 accumulation phase, when the average was 28 $\%_{dcw}$ PHB across repetitions 1, 2 and 3
130 (Fig. 1). This corresponds to an average volumetric productivity of approximately 16
131 $mgPHB \cdot L^{-1} \cdot d^{-1}$ (Table 1). Afterward, PHB content decreased but remained relatively
132 constant (around 24 $\%_{dcw}$ PHB) for the remainder of the accumulation phase (Fig. 1).

133 pH is useful to track biomass activity. During the growth phase of the conditioning period
134 (initially adding 100 $mgIC \cdot L^{-1}$ as bicarbonate), pH fluctuations were anticipated due to
135 photosynthesis and cell respiration, resulting in daytime rises and nighttime drops in pH
136 (Supplementary Fig. 3). Once the pH reached the setpoint (8.5), CO_2 was injected in the
137 PBRs to maintain it in the desired range (Supplementary Fig. 3). While 100 $mgIC \cdot L^{-1}$
138 were present at the start of the conditioning cycle, during repetitions 1-3 bicarbonate was
139 not added. The available IC in the conditioning period enabled more cell grow and;
140 therefore, the increase in pH was faster, resulting in more CO_2 supplied due to pH control
141 (Supplementary Fig. 3). Slower increases in pH during repetitions 1-3 could be attributed
142 to PHB consumption during those growth phases. It is difficult to compare pH trends
143 obtained with those from heterotrophic cultures, since often pH is monitored and
144 controlled[6,19,21,22] but pH profiles from the growth phase (referred to as the "famine
145 phase" in heterotrophic cultures) are rarely available.

146 **Presence of green algae overshadowed PHB production**

147 The same methodology described above was applied to two PBRs inoculated with UP, a
148 microbiome rich in cyanobacteria *Synechococcus* sp. and green algae (Supplementary
149 Fig. 4C and D)[16]. In the conditioning cycle, N (50 $mgN \cdot L^{-1}$) was completely consumed
150 in 25 days (Supplementary Fig. 5), resulting in approximately 550 $mgVSS \cdot L^{-1}$ biomass
151 concentration (Supplementary Fig. 6) and an average specific growth rate of 0.07 d^{-1}
152 (Supplementary Table 1). This rate was relatively lower compared to that obtained with

153 the microbiome R3, richer in cyanobacteria. Subsequent growth phases (repetitions 1, 2
154 and 3) were performed without adding bicarbonate to promote growth of PHB-producers.
155 Green microalgae became noticeable and increased through the experiment, leading to a
156 decrease in the fraction of cyanobacteria in the microbiome population (Supplementary
157 Fig. 7 and 8).

158 Green microalgae have the ability to accumulate Ac as a carbon storage compound in the
159 form of starch or triacylglycerol under N starvation[23,24] and darkness[25]. Therefore, the
160 abundance of these microorganisms in the PBRs possibly increased because during the
161 accumulation phase (when there was no N or light) they could store the added Ac,
162 competing with cyanobacteria for this compound. They would then use it as carbon source
163 during the subsequent growth phase. Additionally, green microalgae could grow using
164 the remaining Ac in the PBRs when changing from phase *i* to *i*+1. Around 150 $mgAc \cdot L^{-1}$
165 remained after 14 days in the accumulation phase of the conditioning cycle
166 (Supplementary Fig. 5), possibly accounting for the substantial rise in green microalgae
167 presence during repetition 1. Their proportion increased from 14 % at the end of
168 conditioning cycle to 75 % at the end of repetition 1, and this ratio remained constant for
169 the remainder of the test (Supplementary Fig. 8).

170 Regarding to PHB production, unlike microbiome R3 that reached a maximum at day 4,
171 microbiome UP followed a very different trend. PHB increased throughout the 14-day
172 accumulation phase, eventually reaching a maximum value of 7 and 8 $\%_{dcw}$ PHB (3 and
173 4 $mgPHB \cdot L^{-1} \cdot d^{-1}$) by the end of the conditioning cycle and repetition 1, respectively
174 (Supplementary Table 1 and Supplementary Fig. 5 and 6). Afterwards, PHB
175 accumulation dropped in repetitions 2 and 3, when only 2 $\%_{dcw}$ PHB was detected at the
176 end of these repetitions (Supplementary Fig. 6), representing less than 1 $mgPHB \cdot L^{-1} \cdot d^{-1}$
177 productivity (Supplementary Table 1). Differences in PHB production among
178 microbiomes, as well as, its sudden decrease were clearly linked to microbiome
179 composition. Microscope observations showed that after repetition 1, green algae were
180 highly present in microbiome UP (Supplementary Fig. 7), whereas such microorganisms
181 were almost undetected in biomass from R3 (Supplementary Fig. 9). Such findings
182 suggested that the presence of microalgae overshadowed the potential production of PHB
183 by the microbiome because green microalgae are non-PHB-producers[17,26,27].

184 **Robustness of cyanobacterial microbiome enables high accumulation of PHB**

185 Microscope observations were conducted at the end of each cycle (conditioning,
186 repetitions 1-3) to assess microbiome composition. Outcomes of microbiome R3 showed
187 that the population remained remarkably consistent (Supplementary Fig. 9). Notably, an
188 average of 93 % of the microbiome comprised two cyanobacteria species, *Synechocystis*
189 sp. and *Synechococcus* sp., indicating a robust and stable microbiome composition in
190 relation to cyanobacteria population (Supplementary Fig. 9). Over the course of the study,
191 both species dominated the culture, although *Synechocystis* sp. was more abundant (60
192 %) than *Synechococcus* sp. (30 %). In addition, presence of green algae decreased during
193 the operation time; in fact, they were not observed in the microscope observations
194 performed (Supplementary Fig. 9).

195 To verify accumulation of PHB by cyanobacteria and no other microorganisms, Nile blue
196 A staining was performed in samples from the end of each cycle (conditioning and
197 repetitions 1-3). PHB was detected using a fluorescence microscope. The positive
198 staining with Nile blue A clearly demonstrated that cyanobacteria were involved in PHB
199 accumulation (Supplementary Fig. 10).

200 Furthermore, the PBRs were operated for one more repetition (repetitions 4). At the end
201 of the starvation phase, biovolume was calculated. Outcomes reveled a dominance of
202 cyanobacteria *Synechocystis* sp. over *Synechoccocus* sp. (Supplementary Fig. 9). Green
203 algae were not observed, suggesting the dominance of PHB accumulators after 108 days
204 of operation under conditions favoring PHB producers.

205 **High intracellular PHB content revealed by TEM**

206 A subsequent cycle (repetition 4) of seven days of growth and seven days under starvation
207 was done with one PBR to obtain images of the intracellular PHB-granules. Samples were
208 collected at three time points: at the start (prior to Ac injection), the fourth day (when
209 maximum biopolymer production occurred) and at end of the starvation phase to monitor
210 its time course. These time points corresponded to days 101, 105 and 108 of the entire
211 experiment, and are referred by those numbers in this section.

212 Biomass used as inoculum was also examined by TEM to observe and compare
213 morphological changes in response to the continuous growth/starvation cycles performed.
214 Inoculum cells, grown in BG-11 medium with 0.5 $mgP \cdot L^{-1}$, displayed a typical
215 cyanobacterial cell organization (Supplementary Fig. 11A), with the thylakoid
216 membranes occupying most of the cytoplasm volume. Small electron-dense glycogen

217 inclusions between the thylakoid layers could be seen. Some cells also presented slightly
218 electron-dense inclusions located close to the thylakoid membranes (Supplementary Fig.
219 11A). These inclusions were not PHB nor polyphosphate granules since GC results
220 revealed that inoculum had no intracellular PHB and both have different morphology and
221 electron density after staining[28,29]. These spherical granules could be presumably
222 carboxysomes and/or lipid bodies.

223 TEM images of samples taken during the accumulation phase revealed distinct electron-
224 transparent inclusion bodies ("white") with a transparent appearance, located near the cell
225 periphery, around the thylakoid membranes. These were attributed to PHB-granules (Fig.
226 5 and Supplementary Fig. 11B). At the phase's onset (before adding Ac, day 101), cells
227 already contained PHB granules because they had experienced 4 cycles of
228 growth/starvation (conditioning + repetitions 1-3), and not all PHB was consumed during
229 the growth phases (Fig. 1 and Supplementary Fig. 11B). In fact, PHB quantifications
230 showed that 15 $\%_{dcw}$ still remained in the biomass (Fig. 2A). Notably, at *Synechocystis*
231 sp. cells exhibited no more than 3 PHB granules at day 101, increasing on day 105 and
232 108 (Fig. 2B). Indeed, the highest PHB accumulation was observed on day 105 (four days
233 after Ac supplementation) (24 $\%_{dcw}$ PHB), with *Synechocystis* sp. presenting a maximum
234 of 6 granules per cell, while *Synechococcus* sp. cells had up to 15 granules (Fig. 2B and
235 C). On day 108, after 7 days in starvation, no differences were detected in the size and
236 number of PHB-granules per cell (Supplementary Fig. 11B) with sample from day 105.
237 Remarkably, relatively similar PHB content was also detected on both days (24 $\%_{dcw}$ PHB
238 on day 105 and 22 $\%_{dcw}$ PHB on day 108) (Fig. 2A). PHB-granules had spherical to oval
239 shape in both cyanobacteria species; but the granules were larger in *Synechocystis* sp.
240 compared to *Synechococcus* sp., with average diameters of 672 ± 83 nm and 217 ± 19
241 nm, respectively. The high degree of variability in both the size and number of
242 biopolymer granules among both species, as well as within cells of the same species,
243 resulted in heterogeneous biopolymer content in the culture (Supplementary Fig. 11B),
244 possibly due to stochastic regulation of PHB synthesis[30].

245 Additionally, processing TEM images by the program ImageJ revealed that cells from
246 samples taken on day 101, 105, and 108 exhibited an estimated biopolymer content of 28
247 $\%_{dcw}$, 35 $\%_{dcw}$ and 20 $\%_{dcw}$, respectively. These approximate values indicate a higher PHB
248 content compared to the results from PHB extraction and quantification by gas

249 chromatography (GC), except for day 108 (15 $\%_{dcw}$, 24 $\%_{dcw}$ and 22 $\%_{dcw}$, for the
250 respective time points).

251 **Expression of key genes involved in PHB metabolism**

252 RT-qPCR was performed to analyze the expression of specific genes encoding key
253 enzymes related to the metabolism of PHB was analysed in repetition 4 of R3 at the same
254 time points in which TEM images were taken by These are the start of the starvation
255 phase (before Ac injection), the fourth day (when maximum biopolymer production
256 occurred), and the end of the starvation phase, corresponding to days 101, 105, and 108
257 of the entire experiment. Additionally, enzymes involved in glycogen metabolism were
258 also analysed since PHB can be synthesized from intracellular glycogen pools[5,31]. Both
259 pathways, as well as the TCA cycle, use Acetyl-CoA, which can be synthesized from Ac,
260 as a primary precursor. Results from day 101 served as reference to compare with
261 outcomes from day 105 and 108 (Supplementary Fig. 12). Note that RT-qPCR targeted
262 *Synechocystis* sp. genes, given their high conservation among species[32], and to their
263 dominance observed in microscope observations (Supplementary Fig. 9).

264 On day 105 (fourth day of the accumulation), the overexpression of genes related to
265 glycogen synthesis (*glgA*, codifying for glycogen synthase), the TCA cycle (*gltA*,
266 codifying for citrate synthase) and PHB synthesis (*phaC*, codifying for
267 polyhydroxyalkanoate synthase) was revealed (Fig. 3A). On day 108 (seventh day of the
268 accumulation), genes *phaC* and *glgp1* (codifying for glycogen phosphorylase, involved
269 in glycogen catabolism) were overexpressed (Fig. 3B). The consistent overexpression of
270 *phaC* on the fourth and seventh days of the starvation period (days 105 and 108
271 respectively) aligns with the observed stable PHB content (24 $\%_{dcw}$ PHB and 22 $\%_{dcw}$
272 PHB, on days 105 and 108 respectively).

273 **PHB characterization**

274 The cyanobacteria-generated polyhydroxyalkanoate was assessed with spectroscopic
275 techniques to make a characterization of the composition of the polymer. As reported in
276 Fig. 4A, main Raman active modes for a reference sample of PHB (PHB-R) were
277 observed at 840 ($\boldsymbol{v}_1$), 1060 ($\boldsymbol{v}_2$), 1300 – 1500 ($\boldsymbol{v}_3$), 1725 ($\boldsymbol{v}_4$) and 2800 – 3100 cm^{-1} ($\boldsymbol{v}_5$)
278 and attributed to C–COO, C–CH_3 stretching, CH_2/CH_3 bending (symmetric and
279 antisymmetric), C=O stretching and different C–H stretching of methyl groups,
280 respectively[33]. Raman spectra comparison between PHB-R and the PHB biogenerated

281 (PHB-B) showed no differences, except from a broad shoulder at 2876 cm^{-1} attributed to
282 impurities acquired during the extraction process (Diamond mark, Fig. 4A). FTIR
283 outcomes (Fig. 4B) corroborated the results obtained by Raman through the observation
284 of the main vibrational modes C–CH_3 stretching, CH_2 wagging and C=O stretching
285 (1057, 1281 and 1724 cm^{-1}, respectively) reported for PHB[33,34]. A broad band at 3000 –
286 4000 cm^{-1} caused by water presence was detected for the PHB-B sample leading to a poor
287 signal-to-noise ratio at the same region.
288
289 Nonetheless, due to significant similarities in Raman and FTIR spectra between PHB and
290 other PHAs, such as poly(3-hydroxybutyrate-co-3-hydroxyvalerate) (PHBHV,
291 Supplementary Fig. 13 and 14), ^{1}H-NMR analysis was deemed necessary to further
292 confirm the sole production of PHB. Careful inspection of the PHB-B NMR spectra (Fig.
293 4C) enabled the peak assignation of the carbons depicted in the PHB monomer (Fig. 4D).

294 **Discussion**

295 Research on PHA production by bacteria is extensive, but studies involving mixed
296 cultures with cyanobacteria are relatively limited. While results on PHB synthesis by
297 cyanobacteria pure cultures have demonstrated their potential as biopolymer producers,
298 current production yields may not yet meet the demands of a market predominantly
299 dominated by petroleum-based plastics. Therefore, efforts to boost their productivity
300 should be pursued.

301 Here we showcase the possibility of sustained PHB synthesis by a cyanobacteria
302 consortium through the application of repetitive biomass growth and PHB accumulation
303 phases. Several key factors contribute to the success of our approach. Firstly, the
304 composition of the microbiome proves crucial for maintaining PHB synthesis over time,
305 with cyanobacteria, the primary PHB producers, requiring dominance in the culture. This
306 strategic control results in notable 25-28 %dcw PHB, ranking among the highest values
307 recorded by the cyanobacteria strains present in the studied community (*Synechocystis*
308 sp. PCC 6803 and *Synechococcus* sp. PCC 6312, Table 2). Although PHB synthesis by
309 *Synechocystis* sp. PCC 6803 has been thoroughly investigated, there is a dearth of
310 literature available on the performance of *Synechococcus* sp. PCC 6312, nor the use of
311 both strains in a mixed culture. Previous studies reporting PHB synthesis usually operated
312 with monocultures under sterile conditions and in very small volumes, rarely exceeding
313 150 mL (Table 2). In the only report of *Synechocystis* sp. PCC 6803 tested in higher

volumes, an engineered strain (ΔSphU) was cultivated with shrimp wastewater in a 15 L PBR22. Despite reporting high intracellular PHB content (Table 2), engineered strains are not optimal for the scale-up of the process in an environmental biotechnology perspective, since production costs will increase due to the requirement of sterile conditions or synthetic substrates.

Our study stands out by demonstrating the use of a microbiome to produce PHB in a 3 L PBR, a notable departure from the other studies done in much lower volume (Table 2). In addition, production remained consistent for an impressive 108-day period, compared to tests lasting less than 2 weeks. This extended duration of steady production attests to the robustness of the culture in accumulating the desired bioproduct. Moreover, it is worth noting that our approach also streamlines operations by utilizing the same PBR for both growth and starvation phases, rather than relying on separate PBRs for each phase, including biomass harvesting steps like centrifugation[35–38]. Here, PBRs have worked under non-sterile conditions in semi-continuous mode, with minimal manipulations, such as Ac addition at the start of each starvation phase and culture purge followed by new medium replacement every 21 days (in fact the purge is the resulting product of our process). This streamlined methodology represents a significant advantage in terms of scalability, reducing both equipment requirements and processing time, ultimately leading to cost savings and increased efficiency.

We also showed that to ensure optimal PHB production, it is imperative to prevent presence of non-PHB producers, like green microalgae, in the initial inoculum. Despite the low P concentration used to prevent their proliferation during growth phases, it became evident that the stored carbon in the form of starch or triacylglycerol and/or the residual Ac significantly contributed to their growth. This indicated that P limitation alone was insufficient to hinder the growth of green microalgae. In a previous study, up to 22 $\%_{dcw}$ PHB was obtained by a microbiome rich in cyanobacteria; nevertheless, production was marked by notable fluctuations due to the presence of green algae[17]. This underscores the critical role of culture composition in achieving stable and reliable PHB production.

Secondly, we provide compelling evidence that cyanobacteria actively accumulate the biopolymer, substantiated by both Nile blue A staining and TEM images. In addition, Nile blue A staining could be used as a rapid and effective methodology to asses PHB synthesis in microbial cultures, aligning with previous reports in sludge from wastewater treatment plants[22,39–41] or the cyanobacteria *Nostoc* sp.[7]. Interestingly, TEM images

347 depicting cyanobacteria cultures with intracellular PHB are not commonly reported. In
348 fact, only a few studies have described the granule size, number or intracellular content
349 in these microorganisms (Supplementary Table 2). Most published works focus on
350 morphological changes between WT and mutant cells, where PHB production was not
351 the main objective[29,42,43]. However, based on the available TEM images, we can conclude
352 that the Synechocystis sp. from our studied mixed culture exhibited one of the highest
353 intracellular biopolymer contents, as well as the greatest number of granules
354 (Supplementary Table 2). Much limited information is found regarding PHB production
355 by *Synechoccocus* sp. From TEM images by[44] and the current study (Fig. 2),
356 *Synechoccocus* sp. presented a higher number of granules, but smaller in size, compared
357 to Synechocystis sp. (Supplementary Table 2).

358 Furthermore, upon processing TEM images by the ImageJ program, we observed a
359 discrepancy between results obtained from PHB extraction from lyophilized biomass and
360 those from image processing. This could be attributed to the larger size and heavier
361 cyanobacterial cells in comparison to heterotrophic bacterial cells[18], leading to incomplete
362 biopolymer extraction; a crucial step prior to GC analysis. Consequently, quantification
363 of PHB content in cyanobacteria tends to be lower. This suggests that the studied
364 microbiome has even greater potential for PHB accumulation, considering the variability
365 in PHB content among cells, as and the underestimation of GC results.

366 Thirdly, the overexpression of gene *phaC* exhibited a direct correlation with increased
367 PHB production during the accumulation phase. PhaC is the key enzyme in PHB
368 synthesis. For instance, *Synechocystis* sp. lacking *phaC* (Δ*phaC*) failed to produce PHB
369 when Ac was added to the medium[45]. In our study, a direct relation between the increase
370 in PHB production (Fig. 2A) and the overexpression of gene *phaC* from day 101 to day
371 105 and 108 was evident (Fig. 3). The overexpression of this gene in the fourth and
372 seventh day of the starvation (days 105 and 108, respectively) was similar, which agrees
373 with the observed constant PHB content (24 $\%_{dcw}$ PHB in day 105 and 22 $\%_{dcw}$ PHB in
374 day 108). This suggested that polymer synthesis from acetate was a relatively fast process
375 since it reached a maximum in four days remaining constant thereafter. In addition to
376 PHB, cyanobacteria also accumulate glycogen as carbon storage compund[5,45]. Outcomes
377 showed that in day 105, glycogen synthesis was underway, as evidenced by the
378 overexpression of *glgA* (Fig. 3A and Supplementary Fig. 12). This gene expression,
379 however, decreased after three days (day 108) (Fig. 3B and Supplementary Fig. 12),

380 indicating that glycogen was the initial storage compound synthesized in response to
381 short-term macronutrient stress conditions, such as nitrogen depletion, as reported by
382 other authors[30,45–47]. Nevertheless, the higher expression of *gltA* on day 105 (Fig. 3A and
383 Supplementary Fig. 12) indicated that part of the Acetyl-CoA was channeled into the
384 TCA cycle instead of being used to produce PHB. Interestingly, this gene was not
385 overexpressed on day 108, suggesting a decrease in carbon flux to TCA, possibly favoring
386 PHB synthesis.

387 On day 108, cells accumulated 22% $_{dcw}$ PHB, as confirmed biopolymer extraction results,
388 and the overexpression of *phaC* (Fig. 2A and Fig. 3B). At this time point, overexpression
389 of genes involved in glycogen synthesis was not detected, further reinforcing the rapid
390 synthesis of glycogen as consequence of nutrients starvation and later PHB accumulation.
391 Additionally, glycogen degradation was active, as indicated by the overexpression of
392 gene *glgp1* (Fig 3B and Supplementary Fig. 12). The stored glycogen was being oxidized
393 due to N-starvation persistence, with degradation products ultimately contributing to the
394 conversion to PHB. This would explain the sustained intracellular PHB content after 7
395 days in starvation by the overexpression of *phaC*, with no observed PHB decrease. These
396 findings agreed with other studies reporting conversion of glycogen to PHB in
397 cyanobacteria[31,46,48]. The degradation of glycogen and its transformation into PHB occurs
398 during prolonged N-starvation to mitigate the potential osmotic impacts of excessive
399 intracellular metabolites accumulation and to generate ATP to maintain basic cellular
400 functions[49,50]. This result elucidated the metabolic dynamics underlying PHB synthesis.

401 Finally, we conducted Raman, FTIR and ^{1}H-NMR analysis to characterize the synthetized
402 biopolymer. Results clearly showed that the biopolymer accumulated by the studied
403 consortium was PHB. While certain cyanobacteria strains are cable of producing co-
404 polymer PHBV[51], absence of peaks with possible attribution to other polymers was
405 observed, providing conclusive evidence for the exclusive synthesis of PHB by
406 *Synechocystis* sp. and *Synechococcus* sp., the cyanobacteria present in the studied
407 microbiome. This conclusion was further supported by additional ^{1}H-NMR
408 measurements conducted on PHB-R and PHBHV (Supplementary Fig. 15 and 16).

409 **Methods**

410 **Inoculum and experimental set-up**

411 Two microbiomes isolated in[16], named R3 and UP, were used as the inoculum for 3 L
412 glass cylindrical photobioreactors (PBRs) of 2.5 L working volume (Supplementary Fig.
413 17). Microbiome sample R3 was collected from the Besòs River (Sant Adrìa de Besòs,
414 Spain, 41°25'20.2"N 2°13'38.2"E), an intermittent Mediterranean stream that receives
415 high amounts of treated wastewater discharged from the sewage treatment plants in the
416 metropolitan area of Barcelona. This microbiome was rich in the unicellular
417 cyanobacteria *Synechocystis* sp. and *Synechococcus* sp. (Supplementary Fig. 4A and B)
418 because of the applied selective pressure described in [16]. These organisms were identified
419 as *Synechocystis* sp. PCC6803 and *Synechococcus* sp. PCC 6312 by phylogenetic analysis
420 based on 16S rRNA gene sequences with the highest similarity, 100 % confidence and
421 97 % confidence, respectively[16]. UP sample was collected from an urban pond located in
422 Diagonal Mar Park (Barcelona, Spain, 41°24'31.0"N 2°12'49.9"E), which is fed with
423 groundwater water. The microbiome was rich in the cyanobacteria *Synechococcus* sp.,
424 identified as *Synechococcus* sp. PCC 6312 with 99 % confidence, and also had green
425 algae (Supplementary Fig. 4C and D).

426 Illumination in reactors was kept at 30 klx (approx. 420 $\mu mol \cdot m^{-2} \cdot s^{-1}$) by 200 W LED
427 floodlight, placed at 15 cm from the reactors surface in 15:9 h light:dark cycles (during
428 growth phase). pH was measured online with a pH probe (HI1001, HANNA instruments,
429 Italy) placed inside the reactors and was controlled at 8 ± 0.5 (during growth phase) by a
430 pH controller (HI 8711, HANNA instruments, Italy). The control system activated an
431 electrovalve which allowed to inject CO_2 inside the reactors when pH reached 8.5. The
432 pH data was saved in a 5 min interval in a computer with the software PC400 (Campbell
433 Scientific). In PHB-accumulation phases (see below) the pH was measured but not
434 controlled in order to avoid IC injection. The pH always maintained in values 7.5 ± 0.5
435 in this phase. PBRs were enclosed in opaque PVC tubes during accumulation phase to
436 ensure dark conditions. Reactors were continuously agitated by a magnetic stirrer
437 ensuring a complete mixing and culture temperature was kept at 30-35 ºC. Two PBRs
438 were used as duplicates.

439 **Experimental strategy**

440 Methodology described in[17] based in cycles of alternation of growth/starvation phases
441 was applied for 108 days (Supplementary Fig. 1). Briefly, experiment started with a
442 conditioning period consisting on a unique cycle with one growth and starvation phases.
443 The growth phase started with the inoculation of the PBR with a biomass concentration

444 of 100 mg volatile suspended solids (VSS)·L^{-1}. BG-11 with modified concentrations of
445 bicarbonate, as source of IC, N and P (100 mgIC L^{-1}, 50 mgN·L^{-1} and 0.1 mgP·L^{-1}) was
446 used as media (Table 3). When N was depleted, the starvation phase began. 600 mg Ac·L^{-}
447 ^{1} was added at this point and PBRs were enclosed with PVC tubes to avoid light
448 penetration.

449 After this first cycle, a total of five cycles were repeated for microbiome R3, and three
450 for UP since microbiome composition led to low PHB synthesis (Supplementary Fig. 6).
451 At the beginning of each cycle, a volume, usually ranging from 800 mL to 1,200 mL, was
452 discarded from the PBRs to purge the culture broth and set approximately 400 mgVSS·L^{-}
453 ^{1} as initial biomass concentration in each cycle. Discarded volume was replaced with new
454 BG-11 medium with 25 mgN·L^{-1}, 0.1 mgP·L^{-1} and without IC to start the growth phase.
455 A daily dose of a solution of KH_2PO_4 was conducted to maintain a certain P concentration
456 inside the reactors (aprox. 0.1 mgP·L^{-1}). Each growth phase lasted seven days, until N
457 was depleted. After that, the starvation phase started with the addition of acetate to reach
458 600 mgAc·L^{-1} in the cultures. All the starvation phases went on for 14 days each; except
459 in repetition 4 with microbiome R3, which only lasted a week.

460 **Analytical methods**

461 At selected times, 50 mL samples were taken from each PBR. Biomass concentration was
462 determined as VSS according to procedures in[52]. Turbidity was measured with
463 turbidimeter (HI93703, HANNA Instruments). For a quick estimation of biomass, VSS
464 and turbidity were correlated by calibration curve (Supplementary Fig. 18).

465 To determine the concentration of dissolved chemical species, samples collected from the
466 reactors were first filtered through a 0.7 µm pore glass microfiber filter. Nitrate and
467 phosphate were quantified following Standard Methods[52]. Note that in BG-11 the only
468 source of N is nitrate. The filtered samples were passed through a 0.45 µm pore size filter
469 a second time to determine Ac (acetate) by ion chromatography (CS-1000, Dionex
470 Corporation, USA).

471 **Microscopy**

472 Biomass composition was tracked at the end of each cycle through the use of bright light
473 and fluorescence microscopy observations (Eclipse E200, Nikon, Japan). Cyanobacteria
474 and green algae were identified and classified based on morphological descriptions[53,54].
475 Cell counting was done in a Neubauer chamber at the end of each starvation phase.

476 Individual cells were counted until reach >400 cells to minimize the margin error to less
477 than 10 %[55].

478 Intracellular PHB in the biomass was observed by staining cells. Small aliquots of
479 samples from the reactors were heat-fixed on glass slides and stained with 1% Nile Blue
480 for 10 min at room temperature. Excess dye was removed with distilled water. 8% acetic
481 acid solution was applied for 1 min at room temperature, washed with distilled water and
482 the slide was allowed to air dry. The stained samples were examined under fluorescence
483 microscopy at excitation and emission wavelength of 510 nm and 590 nm, respectively.

484 **Transmission Electron Microscope**

485 At the start of the starvation phase (prior to Ac injection), the fourth day and at the end
486 of the starvation phase in repetition 4, 4 mL samples from the reactors were centrifuged
487 (2,000 rpm, 10 min). The supernatant was discarded and the pellet was resuspended in
488 fixative 2% paraformaldehyde and 2.5% glutaraldehyde in 0.1 M PB. Fixation was done
489 at room temperature for 2 h. Then, cells were washed four times in 0.1 M PB. Fixed
490 material was subjected to osmification for 3 h at 4 ºC. After that time, samples were
491 washed four times with MilliQ water and stored in 0.1M PB buffer at 4 ºC. Samples were
492 dehydrated through a graded ethanol series at 4 ºC and gentle agitation (one change of 10
493 min in 50 % ethanol, two changes of 10 min each in 70, 90 and 96 % ethanol and three
494 changes of 15 min each in 100% ethanol). Samples were embedded using EPON 812
495 resin kit molds and left 72 h in silicon molds in an oven at 60 ºC to polymerize. Ultra-
496 thin sections (100 nm) were cut on a SORVALL MT2-B ultramicrotome with a Diatome
497 45 º diamond blade, collected on Formvar-coated 300-mesh coper grids and left to dry 15
498 h. Finally, samples were stained with UA-zero® and 3 % lead citrate and left to dry 12 h.
499 The sections were examined in a PHILLIPS TECNAI-10 electron microscope operated
500 at 100 kV.

501 **Image processing and analysis**

502 Image analysis was performed using FIJI-ImageJ software. TEM images corresponding
503 to different time points (day 101, 105, and 108) during the accumulation phase of
504 repetition 4 were utilized to measure the size of PHB granules produced in each strain.
505 Prior to measurement, the TEM images were calibrated using a scalebar and the arrow
506 tool to obtain accurate dimensions of the PHB granules. For calculating the approximate
507 percentage of PHB, the TEM images were first segmented to obtain two black and white

508 images: (i) a mask representing the cell area, and (ii) a mask containing the PHB granules.
509 To calculate the area of (i) cells and (ii) PHB granules, image analysis was applied using
510 the measurements tool. Subsequently, the percentage of PHB granules was computed by
511 dividing the number of pixels in the PHB granule mask by the number of pixels in the
512 cell area mask.

513 **RNA extraction and quantitative real-time PCR**

514 In repetition 4, samples were collected at the start (prior to Ac injection), the fourth day
515 and at the end of the starvation phase. Methodology was adapted from[46]. Fresh biomass
516 (10 mL) was harvested by centrifugation at 14,000 rpm for 5 min at 4 ºC and stored at –
517 80 ºC in an ultra-freezer (Arctiko, Denmark). Frozen cells were homogenized in lysis
518 buffer and TRIzol followed by Bead Beating for cell lysis. Afterward, RNA was isolated
519 using the PureLink RNA Mini Kit (Ambion, Thermo fisher Scientific, Waltham, USA)
520 following the manufacturer's recommendations. The purified RNA was quantified using
521 a Take3 microvolume plate (Synergy HTX, Agilent, USA). The RNA was reverse
522 transcribed using the RevertAidTM Kit (ThermoFisher Scientific, USA) using 100 ng of
523 total RNA according to manufacturer's protocol with a combination of the provided oligo
524 (dT) and random hexamer primers (20 µL). The quality and quantity of the cDNA
525 fragments was analyzed using a Take3 microvolume plate (Synergy HTX, Agilent, USA).

526 Gene expression levels were determined using the qPCR thermocycler Quantstudio 3
527 (ThermoFisher Scientific, USA). To do this, designed primers described in[46] at 300 nM
528 and the Powerup SYBR master mix (ThermoFisher Scientific, USA) were used. The 16S
529 RNA was selected as the housekeeping gene as the one with lower variability between
530 the different tested conditions. For the results, the mean Ct values were determined using
531 the method from[56] by calculating the average of the triplicate measurements for each
532 condition and gene. The ΔCt was calculated by subtracting the mean Ct value of the
533 housekeeping gene from the mean Ct value of the gene of interest. ΔΔCt is the difference
534 between ΔCt of the day 3, and 7 of accumulation and the ΔCt of day 1 (before adding Ac)
535 as control Ct values. Finally, to calculate the relative fold gene expression level, 2 to the
536 power of negative ΔΔCt according to equation 1:

$$\text{Fold gene expression} = 2^{-(\Delta\Delta Ct)} \quad (1)$$

537 Statistical analysis was performed by one-way ANOVA to evaluate the possible
538 interaction between genes. P-values lower than 5 % were considered statistically
539 significant.

540 **PHB extraction and quantification**

541 PHB analysis was done for samples collected during starvation phases for both
542 microbiomes. Methodology was adapted from described in [57]. Concisely, 50 mL of mixed
543 liquor were collected and centrifuged (4,200 rpm, 7.5 min), frozen at −80 °C overnight
544 in an ultra-freezer (Arctiko, Denmark) and finally freeze-dried for 24 h in a freeze dryer
545 (−110 ºC, 0.05 hPa) (Scanvac, Denmark). 3-3.5 mg of freeze-dried biomass were mixed
546 with 1 mL CH_3OH with H_2SO_4 (20% v/v) and 1 mL $CHCl_3$ containing 0.05 % w/w
547 benzoic acid. Samples were heated for 5 h at 100 ºC in a dry-heat thermo-block (Selecta,
548 Spain). Then, they were placed in a cold-water bath for 30 min to ensure they were cooled.
549 After that, 1 mL of deionized water was added to the tubes and they were vortexed for 1
550 min. $CHCl_3$ phase, containing PHB dissolved, was recovered with a glass pipette and
551 introduced in a chromatography vial containing molecular sieves. Samples were analysed
552 by gas chromatography (GC) (7820A, Agilent Technologies, USA) using a DB-WAX
553 125-7062 column (Agilent Technologies, USA). Helium was used as the gas carrier (4.5
554 $mL \cdot min^{-1}$). Injector had a split ratio of 5:1 and a temperature of 230 °C. FID had a
555 temperature of 300 °C. A standard curve of the co-polymer PHB-HV was used to quantify
556 the PHB content.

557 **PHB characterization**

558 Raman spectra of the samples were acquired using an inVia Qontor confocal Raman
559 microscope (Renishaw) equipped with a Renishaw Centrus 2957T2 detector and a 785
560 nm laser. All the measurements were performed in mapping mode (64 points) to ensure
561 obtention of representative data. FTIR vibrational studies were recorded on a FTIR
562 Nicolete 6700 spectrometer through a SmartOrbit ATR accessory with Ge crystal and
563 DTGS/CsI detector. Each sample measurement was performed between 4000 – 675 cm^{-1}
564 with a 2 cm^{-1} resolution and spectra processing was carried out using the OMNIC
565 Spectroscopy software. The synthesized polymer and references were analysed through
566 ^{1}H-NMR spectroscopy; using a Bruker Avance III-400 spectrometer operating at 400.1
567 MHz. The chemical shift was calibrated using tetramethylsilane as internal standard and

568 the samples were dissolved in deuterated chloroform ($CDCl_3$). Recording of 256 scans
569 was performed for all samples.

570 **Calculations**

571 Total biovolumes (BV) in $mm^3 \cdot L^{-1}$ of each species (cyanobacteria (*Synechocystis* sp. and
572 *Synechococcus* sp.) and the green microalgae) were calculated using the formula:

573 $$BV = \frac{n \cdot V}{10^6} \quad (2)$$

574 where n is the number of cells counted in a sample ($cells \cdot L^{-1}$) and V is the average volume
575 of each species (μm^3). 10^6 is a factor conversion from $\mu m^3 \cdot mL^{-1}$ to $mm^3 \cdot L^{-1}$. Cell volume
576 was calculated by volumetric equations of geometric shape closest to the cells of each
577 species. Volume equations of sphere, cylinder and ellipsoid were used for BV calculation
578 of *Synechocystis* sp., *Synechococcus* sp. and green algae, respectively (Supplementary
579 Table 3). Cell dimensions (length and width) were obtained from images of microscope
580 observations (software NIS- Element viewer®).

581 Kinetic coefficients were calculated as follows:

582 Specific growth rate (d^{-1}) was calculated using the general formula

583 $$\mu_X = \frac{\ln(x)_{ti} - \ln(x)_{t0}}{t_i - t_o} \quad (3)$$

584 where $\ln(X)_{ti}$ and $\ln(X)_{tn}$ are the natural logarithms of the biomass concentration
585 ($mgVSS \cdot L^{-1}$) at experimental day (t_i) and at the beginning of the growth phase (t_0),
586 respectively. t_i values were considered as the day when biomass concentration reached
587 stationary phase).

588 Biomass volumetric production rate ($mg \cdot L^{-1} \cdot d^{-1}$) was calculated as:

589 $$r_X = \frac{X_{ti} - X_{to}}{t_i - t_0} \quad (4)$$

590 where X_{ti} ($mg \cdot L^{-1}$) and X_{t0} ($mg \cdot L^{-1}$) are the biomass concentration (in $mgVSS \cdot L^{-1}$) at time
591 t_i (when biomass reached stationary phase) and at the beginning of the growth phase (t_0).
592 *i* is the total number of days that the growth phase lasted.

593 The nitrogen (N) to biomass (X) yield was calculated only during the growth phase by:

594 $$Y_{X/N} = \frac{VSS_{ti} - VSS_{t0}}{N_{ti} - N_{t0}} \quad (5)$$

where VSS_{ti} ($mg \cdot L^{-1}$) and VSS_{t0} ($mg \cdot L^{-1}$) are the biomass concentration at the end (t_i) and at the start of the phase (t_0). N_{ti} ($mg \cdot L^{-1}$) and N_{t0} ($mg \cdot L^{-1}$) are the nitrogen concentration ($N\text{-}NO_3^-$) at the end and at the beginning of each growth phase, respectively.

The specific consumption rate of nitrogen ($mgN \cdot mgVSS^{-1} \cdot d^{-1}$) was calculated as:

$$q_{N-NO3} = \frac{\mu_X}{Y_{X/N}} \quad (6)$$

where μ_X was obtained as shown in equation 3 and $Y_{X/N}$ in equation 5.

PHB volumetric production rate (Υ_{PHB} ($mgPHB \cdot L^{-1} \cdot d^{-1}$)) was obtained by:

$$\Upsilon_{PHB} = \frac{(\%_{dcw}PHB_{ti} \cdot X_{ti} - \%_{dcw}PHB_{t0} \cdot X_{t0})/100}{t_i - t_0} \quad (7)$$

where $\%_{dcw}PHB_{ti}$ and $\%_{dcw}PHB_{t0}$ are the percentage of PHB respect biomass quantified at time *i* (end of accumulation phase) and at the beginning of the accumulation phase (t_0). X_{ti} and X_{to} are the biomass concentration (in $mgVSS \cdot L^{-1}$) at the beginning (t_0) and end of the accumulation phase (t_i).

The PHB yield on acetate (Ac) ($Y_{PHB/Ac}$) was calculated on a COD-basis by:

$$Y_{PHB/Ac} = \frac{PHB_{ti} - PHB_{t0}}{600 - Ac_{ti}} \quad (8)$$

The amount of PHB produced (given as chemical oxygen demand (COD): 1.67 $gCOD \cdot gPHB^{-1}$) was obtained by multiplying the $\%_{dcw}$ PHB produced per biomass concentration (in $mgVSS \cdot L^{-1}$) at time *i* (experimental day) and at the beginning (t_0) of the accumulation phase. Ac_{ti} ($mg \cdot L^{-1}$) is the acetate concentration (given 1.07 $gCOD \cdot gAc^{-1}$) at the experimental day (t_i) of the starvation phase. 600 $mgAc \cdot L^{-1}$ is the amount of added acetate.

References

1. Senatore, V. *et al.* Production of phycobiliproteins, bioplastics and lipids by the cyanobacteria Synechocystis sp. treating secondary effluent in a biorefinery approach. *Sci. Total Environ.* **857**, (2023).

2. Yashavanth, P. R., Das, M. & Maiti, S. K. Recent progress and challenges in cyanobacterial autotrophic production of polyhydroxybutyrate (PHB), a bioplastic. *J. Environ. Chem. Eng.* **9**, (2021).

623 3. Pagels, F., Guedes, A. C., Amaro, H. M., Kijjoa, A. & Vasconcelos, V.
624 Phycobiliproteins from cyanobacteria: Chemistry and biotechnological
625 applications. *Biotechnol. Adv.* **37**, 422–443 (2019).

626 4. Chen, G.-Q. Industrial Production of PHA. **14**, 121–132 (2010).

627 5. Rueda, E. *et al.* Polyhydroxybutyrate and glycogen production in
628 photobioreactors inoculated with wastewater borne cyanobacteria monocultures.
629 *Bioresour. Technol.* **295**, 122233 (2020).

630 6. Rueda, E., Altamira-Algarra, B. & García, J. Process optimization of the
631 polyhydroxybutyrate production in the cyanobacteria Synechocystis sp. and
632 Synechococcus sp. *Bioresour. Technol.* **356**, 127330 (2022).

633 7. Ansari, S. & Fatma, T. Cyanobacterial Polyhydroxybutyrate (PHB): Screening,
634 Optimization and Characterization. *PLoS One* **11 (6)**, (2016).

635 8. Monshupanee, T. & Incharoensakdi, A. Enhanced accumulation of glycogen,
636 lipids and polyhydroxybutyrate under optimal nutrients and light intensities in the
637 cyanobacterium Synechocystis sp. PCC 6803. *J. Appl. Microbiol.* **116**, 830–838
638 (2014).

639 9. Panda, B., Jain, P., Sharma, L. & Mallick, N. Optimization of cultural and
640 nutritional conditions for accumulation of poly-β-hydroxybutyrate in
641 Synechocystis sp. PCC 6803. *Bioresour. Technol.* **97**, 1296–1301 (2006).

642 10. Khetkorn, W., Incharoensakdi, A., Lindblad, P. & Jantaro, S. Enhancement of
643 poly-3-hydroxybutyrate production in Synechocystis sp. PCC 6803 by
644 overexpression of its native biosynthetic genes. *Bioresour. Technol.* **214**, 761–
645 768 (2016).

646 11. Simonazzi, M. *et al.* Production of polyhydroxybutyrate by the cyanobacterium
647 cf. Anabaena sp. *Int. J. Biol. Macromol.* **191**, 92–99 (2021).

648 12. Panda, B. & Mallick, N. Enhanced poly-b-hydroxybutyrate accumulation in a
649 unicellular cyanobacterium, Synechocystis sp. PCC 6803. *Lett. Appl. Microbiol.*
650 **44**, 194–198 (2007).

651 13. Estévez-Alonso, Á. *et al.* Calcium enhances polyhydroxyalkanoate production
652 and promotes selective growth of the polyhydroxyalkanoate-storing biomass in

653 municipal activated sludge. *Water Res.* **226**, 119259 (2022).

654 14. Crognale, S. *et al.* Effect of the organic loading rate on the PHA-storing
655 microbiome in sequencing batch reactors operated with uncoupled carbon and
656 nitrogen feeding. *Sci. Total Environ.* **825**, (2022).

657 15. Arias, D. M. *et al.* Polymer accumulation in mixed cyanobacterial cultures
658 selected under the feast and famine strategy. *Algal Res.* **33**, 99–108 (2018).

659 16. Altamira-Algarra, B. *et al.* New strategy for bioplastic and exopolysaccharides
660 production: Enrichment of field microbiomes with cyanobacteria. *bioRxiv*
661 2023.05.30.542819 (2023) doi:10.1101/2023.05.30.542819.

662 17. Altamira-Algarra, B., Lage, A., García, J. & Gonzalez-Flo, E. Species
663 composition determines bioplastics production in photosynthetic microbiomes:
664 strategy to enrich cyanobacteria PHB-producers. *bioRxiv* 2023.05.30.542808
665 (2023) doi:10.1101/2023.05.30.542808.

666 18. Sudesh, K., Taguchi, K. & Doi, Y. Effect of increased PHA synthase activity on
667 polyhydroxyalkanoates biosynthesis in Synechocystis sp. PCC6803. *Int. J. Biol.*
668 *Macromol.* **30**, 97–104 (2002).

669 19. Rueda, E., Gonzalez-Flo, E., Roca, L., Carretero, J. & Garciá, J. Accumulation of
670 polyhydroxybutyrate in Synechocystis sp. isolated from wastewaters: Effect of
671 salinity, light, and P content in the biomass. *J. Environ. Chem. Eng.* **10**, 107952
672 (2022).

673 20. Third, K. A., Burnett, N. & Cord-Ruwisch, R. Simultaneous nitrification and
674 denitrification using stored substrate (PHB) as the electron donor in an SBR.
675 *Biotechnol. Bioeng.* **83**, 706–720 (2003).

676 21. Burniol-Figols, A. *et al.* Polyhydroxyalkanoates (PHA) production from
677 fermented crude glycerol: Study on the conversion of 1,3-propanediol to PHA in
678 mixed microbial consortia. *Water Res.* **128**, 255–266 (2018).

679 22. Carvalheira, M. *et al.* Valorization of Brewery Waste through
680 Polyhydroxyalkanoates Production Supported by a Metabolic Specialized
681 Microbiome. *Life* **12**, 1–14 (2022).

682 23. Fan, J. *et al.* Oil accumulation is controlled by carbon precursor supply for fatty

683 acid synthesis in Chlamydomonas reinhardtii. *Plant Cell Physiol.* **53**, 1380–1390
684 (2012).

685 24. Bogaert, K. A. *et al.* Metabolic, physiological, and transcriptomics analysis of
686 batch cultures of the green microalga Chlamydomonas grown on different acetate
687 concentrations. *Cells* **8**, 1–21 (2019).

688 25. Turon, V., Trably, E., Fayet, A., Fouilland, E. & Steyer, J. P. Raw dark
689 fermentation effluent to support heterotrophic microalgae growth: Microalgae
690 successfully outcompete bacteria for acetate. *Algal Res.* **12**, 119–125 (2015).

691 26. Arias, D. M., Uggetti, E., García-Galán, M. J. & García, J. Cultivation and
692 selection of cyanobacteria in a closed photobioreactor used for secondary effluent
693 and digestate treatment. *Sci. Total Environ.* **587–588**, 157–167 (2017).

694 27. Fradinho, J. C., Oehmen, A. & Reis, M. A. M. Effect of dark/light periods on the
695 polyhydroxyalkanoate production of a photosynthetic mixed culture. *Bioresour.*
696 *Technol.* **148**, 474–479 (2013).

697 28. Tsang, T. K., Roberson, R. W. & Vermaas, W. F. J. Polyhydroxybutyrate
698 particles in Synechocystis sp. PCC 6803: Facts and fiction. *Photosynth. Res.* **118**,
699 37–49 (2013).

700 29. Solovchenko, A. *et al.* Phosphorus Feast and Famine in Cyanobacteria: Is Luxury
701 Uptake of the Nutrient Just a Consequence of Acclimation to Its Shortage? *Cells*
702 **9**, (2020).

703 30. Koch, M., Orthwein, T., Alford, J. T. & Forchhammer, K. The Slr0058 Protein
704 From Synechocystis sp. PCC 6803 Is a Novel Regulatory Protein Involved in
705 PHB Granule Formation. *Front. Microbiol.* **11**, 1–13 (2020).

706 31. Koch, M., Doello, S., Gutekunst, K. & Forchhammer, K. PHB is produced from
707 glycogen turn-over during nitrogen starvation in Synechocystis sp. PCC 6803.
708 *Int. J. Mol. Sci.* **20**, (2019).

709 32. Hai, T., Hein, S. & Steinbüchel, A. Multiple evidence for widespread and general
710 occurrence of type-III PHA synthases in cyanobacteria and molecular
711 characterization of the PHA synthases from two thermophilic cyanobacteria:
712 Chlorogloeopsis fritschii PCC 6912 and Synechococcus sp. strain MA1.

713 *Microbiology* **147**, 3047–3060 (2001).

714 33. Izumi, C. M. S. & Temperini, M. L. A. FT-Raman investigation of biodegradable
715 polymers: Poly(3-hydroxybutyrate) and poly(3-hydroxybutyrate-co-3-
716 hydroxyvalerate). *Vib. Spectrosc.* **54**, 127–132 (2010).

717 34. Bayari, S. & Severcan, F. FTIR study of biodegradable biopolymers: P(3HB),
718 P(3HB-co-4HB) and P(3HB-co-3HV). *J. Mol. Struct.* **744–747**, 529–534 (2005).

719 35. Mariotto, M., Egloff, S., Fritz, I. & Refardt, D. Cultivation of the PHB-producing
720 cyanobacterium Synechococcus leopoliensis in a pilot-scale open system using
721 nitrogen from waste streams. *Algal Res.* **70**, 103013 (2023).

722 36. Koch, M. *et al.* Maximizing PHB content in Synechocystis sp. PCC 6803: a new
723 metabolic engineering strategy based on the regulator PirC. *Microb. Cell Fact.*
724 **19**, 1–12 (2020).

725 37. Gracioso, L. H. *et al.* Light excess stimulates Poly-beta-hydroxybutyrate yield in
726 a mangrove-isolated strain of Synechocystis sp. *Bioresour. Technol.* **320**, 1–7
727 (2021).

728 38. Troschl, C. *et al.* Pilot-scale production of poly-β-hydroxybutyrate with the
729 cyanobacterium Synechocytis sp. CCALA192 in a non-sterile tubular
730 photobioreactor. *Algal Res.* **34**, 116–125 (2018).

731 39. Oshiki, M. ., Satoh, H. . & Mino, T. Rapid quantification of
732 polyhydroxyalkanoates (PHA) concentration in activated sludge with the
733 fluorescent dye Nile blue A. *Water Sci. Technol.* **64 (3)**, 747–753 (2011).

734 40. Sruamsiri, D., Thayanukul, P. & Suwannasilp, B. B. In situ identification of
735 polyhydroxyalkanoate (PHA)-accumulating microorganisms in mixed microbial
736 cultures under feast/famine conditions. *Sci. Rep.* **10**, 1–10 (2020).

737 41. Mesquita, D. P. *et al.* Polyhydroxyalkanoate granules quantification in mixed
738 microbial cultures using image analysis : Sudan Black B versus Nile Blue A
739 staining. *Anal. Chim. Acta* **865**, 8–15 (2015).

740 42. Nagarajan, S., Srivastava, S. & Sherman, L. A. Essential role of the plasmid
741 hik31 operon in regulating central metabolism in the dark in Synechocystis sp.
742 PCC 6803. *Mol. Microbiol.* **91**, 79–97 (2014).

743 43. Klotz, A. *et al.* Awakening of a Dormant Cyanobacterium from Nitrogen
744 Chlorosis Reveals a Genetically Determined Program. *Curr. Biol.* **26**, 2862–2872
745 (2016).

746 44. Asada, Y., Miyake, M., Miyake, J., Kurane, R. & Tokiwa, Y. Photosynthetic
747 accumulation of poly-(hydroxybutyrate) by cyanobacteria - The metabolism and
748 potential for CO2 recycling. *Int. J. Biol. Macromol.* **25**, 37–42 (1999).

749 45. Damrow, R., Maldener, I. & Zilliges, Y. The multiple functions of common
750 microbial carbon polymers, glycogen and PHB, during stress responses in the
751 non-diazotrophic cyanobacterium Synechocystis sp. PCC 6803. *Front.*
752 *Microbiol.* **7**, 1–10 (2016).

753 46. Rueda, E. *et al.* Inorganic carbon stimulates the metabolic routes related to the
754 polyhdroxybutyrate production in a Synechocystis sp. strain (cyanobacteria)
755 isolated from wastewater. *Sci. Total Environ.* **829**, (2022).

756 47. Forchhammer, K. & Schwarz, R. Nitrogen chlorosis in unicellular cyanobacteria
757 – a developmental program for surviving nitrogen deprivation. *Environ.*
758 *Microbiol.* **21**, 1173–1184 (2019).

759 48. Kamravamanesh, D. *et al.* Increased poly-B-hydroxybutyrate production from
760 carbon dioxide in randomly mutated cells of cyanobacterial strain Synechocystis
761 sp. PCC 6714: Mutant generation and characterization. *Bioresour. Technol.* **266**,
762 34–44 (2018).

763 49. Henderson, R. A. & Jones, C. W. Physiology of poly-3-hydroxybutyrate (PHB)
764 production by Alcaligenes eutrophus growing in continuous culture.
765 *Microbiology* **143**, 2361–2371 (1997).

766 50. Thiel, K. *et al.* Redirecting photosynthetic electron flux in the cyanobacterium
767 Synechocystis sp. PCC 6803 by the deletion of flavodiiron protein Flv3. *Microb.*
768 *Cell Fact.* **18**, 1–16 (2019).

769 51. Tarawat, S., Incharoensakdi, A. & Monshupanee, T. Cyanobacterial production
770 of poly(3-hydroxybutyrate-co-3-hydroxyvalerate) from carbon dioxide or a single
771 organic substrate: improved polymer elongation with an extremely high 3-
772 hydroxyvalerate mole proportion. *J. Appl. Phycol.* **32**, 1095–1102 (2020).

52. Amerian Public Health Association. *Standard Methods for the Examination of Water and Wastewater*. (2012).

53. Komárek, J., Kaštovský, J. & Jezberová, J. Phylogenetic and taxonomic delimitation of the cyanobacterial genus aphanothece and description of anathece gen. nov. *Eur. J. Phycol.* **46**, 315–326 (2011).

54. Komárek, J., Johansen, J. R., Šmarda, J. & Strunecký, O. Phylogeny and taxonomy of synechococcus–like cyanobacteria. *Fottea* **20**, 171–191 (2020).

55. P, A. & J, T. Estimating cell numbers. in *Manual on Harmful Marine Microalgae* (eds. G.M., H., D.M., A. & A.D., C.) 99–129 (UNESCO, 2004).

56. Bustin, S. A. A-Z of Quantitative PCR. in (ed. International University Line) 87–112 (2004).

57. Lanham, A. B. *et al.* Determination of the extraction kinetics for the quantification of polyhydroxyalkanoate monomers in mixed microbial systems. *Process Biochem.* **48**, 1626–1634 (2013).

58. Tanweer, S. & Panda, B. Prospect of Synechocystis sp. PCC 6803 for synthesis of poly(3-hydroxybutyrate-co-4-hydroxybutyrate). *Algal Res.* **50**, 101994 (2020).

59. Krasaesueb, N., Incharoensakdi, A. & Khetkorn, W. Utilization of shrimp wastewater for poly-β-hydroxybutyrate production by Synechocystis sp. PCC 6803 strain ΔSphU cultivated in photobioreactor. *Biotechnol. Reports* **23**, e00345 (2019).

60. Krasaesueb, N., Promariya, A., Raksajit, W. & Khetkorn, W. Inactivation of phosphate regulator (SphU) in cyanobacterium Synechocystis sp. 6803 directly induced acetyl phosphate pathway leading to enhanced PHB level under nitrogen-sufficient condition. *J. Appl. Phycol.* **33**, 2135–2144 (2021).

61. Carpine, R. *et al.* Genetic engineering of Synechocystis sp. PCC6803 for poly-β-hydroxybutyrate overproduction. *Algal Res.* **25**, 117–127 (2017).

Acknowledgements

This research was supported by the European Union's Horizon 2020 research and innovation programme under the grant agreement No 101000733 (project PROMICON). B.A.A. thanks the Agency for Management of University and Research (AGAUR) for her grant [FIAGAUR_2021]. E.G.F. would like to thank the European Union-NextGenerationEU, Ministry of Universities and Recovery, Transformation and Resilience Plan for her research grant [2021UPF-MS-12]. J.G. acknowledges the support provided by the ICREA Academia program.

Author contributions

Conceptualization and experimental design by B.A.A., J.G. and E.G.F.; experimental work by B.A.A., A.L., A.L.M and M.A.; data analysis by B.A.A. and M.A.; writing – draft preparation by B.A.A. and M.A.; review and editing by J.G. and E.G.F.; project administration and funding acquisition by J.G. and E.G.F.

Competing interests

The authors declare no competing interests.

Materials & Correspondence

Correspondence and material requests should be addressed to Joan Garcia.

Tables Display items

Table 1. Average of the kinetic and stoichiometric parameters obtained during growth and accumulation phase of each cycle. Values presented in growth phase were measured when biomass reached stationary phase (see Fig. 1). Values in accumulation phase are the average value form both PBRs when the highest PHB content (%dcw) was obtained (at day 8 of accumulation phase in conditioning cycle; day 4 of accumulation phase in repetitions 1 and 2; and day 3 of accumulation phase in repetition 3).

Growth phase				
	Conditioning	**Repetition**		
		1	**2**	**3**
VSS ($mg \cdot L^{-1}$)	802 ± 0.04	807 ± 0.09	818 ± 0.11	650 ± 0.05
μ (d^{-1})	0.52	0.17	0.18	0.16
$\Upsilon_{biomass}$ ($mgVSS \cdot L^{-1} \cdot d^{-1}$)	175.41	100	104.51	83.33
q_N($mgN \cdot gVSS \cdot d^{-1}$)	37.08	6.59	6.39	9.3
$Y_{X/N}$	14.03	16	16.72	10
Accumulation phase				

	Conditioning	Repetition		
		1	2	3
PHB (%dcw)	27 ± 2	27 ± 1	26± 3	28 ± 2
Υ_{PHB} (mgPHB·L^{-1}·d^{-1})	13.55 ± 0.24	15.79 ± 0.47	17.02 ± 0.65	19.74 ± 0.35
$Y_{PHB/Ac}$ (g PHBCOD/g AcCOD)	0.08 ± 0.02	1.14 ± 0.02	n.d.	n.d.

n.d. stands for no data.

Table 2. Comparison of PHB production with *Synechocystis* sp. PCC6803.

Genotype	Working volume (L)	Culture conditions	Accumulation time (days)	PHB fraction (%dcw)	Reference
WT	0.1	N-, P- & Ac+	21	33	[58]
WT (microbiome)	3	N-, P- & Ac+	14*	27	This study
WT	0.05	P- & Ac+	14	26	[9]
WT	0.05	N-, P- & Ac+	20	20	[36]
WT	0.15	N-, P- & Glc+	12	13	[8]
ΔPirC and OE PhaAB (*Cupriavidus necator*)	0.05	N-, P- & Ac+	20	81	[36]
ΔPirC and OE PhaAB (*Cupriavidus necator*)	0.05	N- & P-	20	63	[36]
OE PhaAB (native)	0.05	N- & Ac+	9	35	[10]
ΔSphU	15	Shrimp wastewater	11	33	[59]
ΔSphU	0.05	N+	14	15	[60]
OE Xfpk	0.08	N- & P-	30	12	[61]
OE PhaAB (*Cupriavidus necator*)	0.05	N- & Ac+	8	11	[18]

WT: wild-type; OE: overexpression; Δ: deletion; PirC: PII-interacting regulator; PhaA: beta-ketothiolase; PhaB: acetoacetyl-CoA reductase; SphU: phosphate regulator; Xfpk: phosphoketolase; N: Nitrogen; P: Phosphorus; Ac: Acetate; Glc: Glucose; -: defficiency; +: supplementation. *Note that all references are batch experiments, while in this study, three iterated accumulation phases have been performed with the same culture biomass, representing a total of 94 days of reactor operation.

Table 3. Culture conditions.

Period	Phase	IC (mg·L^{-1})	N (mg·L^{-1})	P (mg·L^{-1})	Ac (mg·L^{-1})	Lightness (h of light:dark)
Conditioning	Growth	100	50	0.1	-	15:09
	Starvation	-	-	-	600	0
Repetitions	Growth	-	25	0.1	-	15:09
	Starvation	-	-	-	600	0

Figures

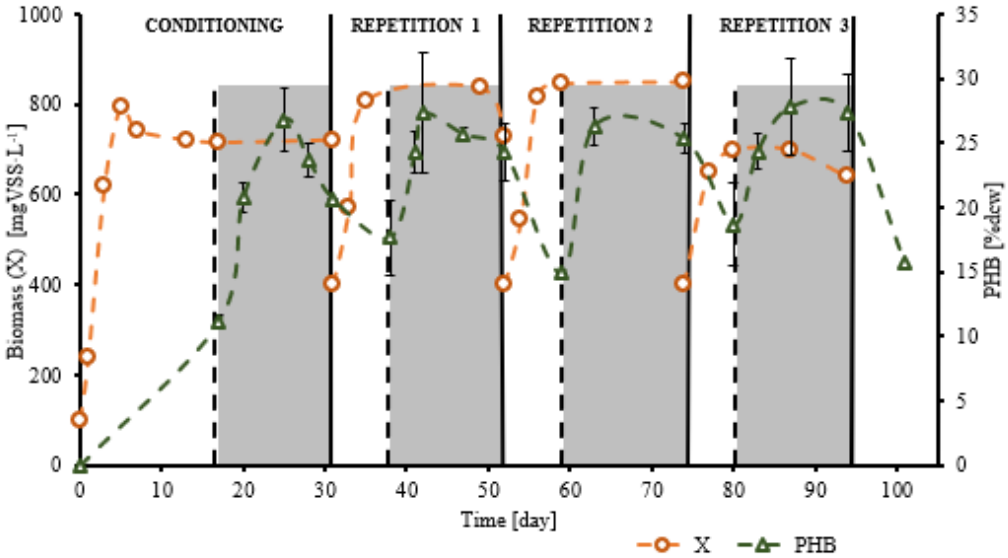

Figure 1. Average biomass (as VSS) and PHB evolution in PBR 1 & 2 of the microbiome R3 for conditioning cycle and repetitions 1-3. Error bars indicate the standard deviation of the replicates. Dashed vertical lines indicate the beginning of starvation phase and vertical continuous black lines illustrate end of cycle (conditioning/repetition). Values of biomass were estimated from turbidity measurements. PHB was not measured in growth phase of each cycle.

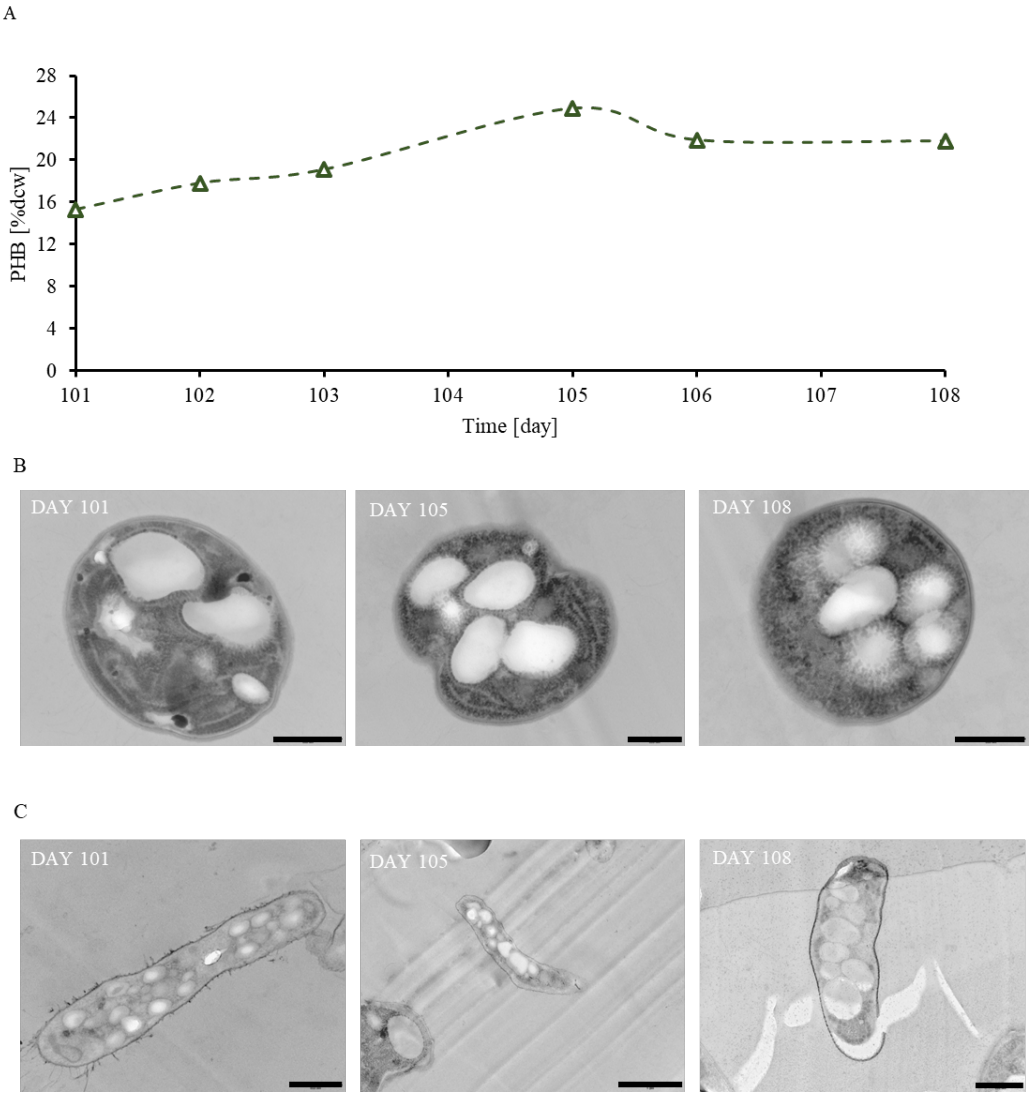

Figure 2. (A) Evolution of PHB production. TEM images of (B) *Synechocystis* sp. and (C) *Synechoccocus* sp. from repetition 4. PHB granules are visible as white inclusions inside the cell. Scale bar is 500 nm for all photos, except for photo (C) day 108, in which scale bar is 1 µm.

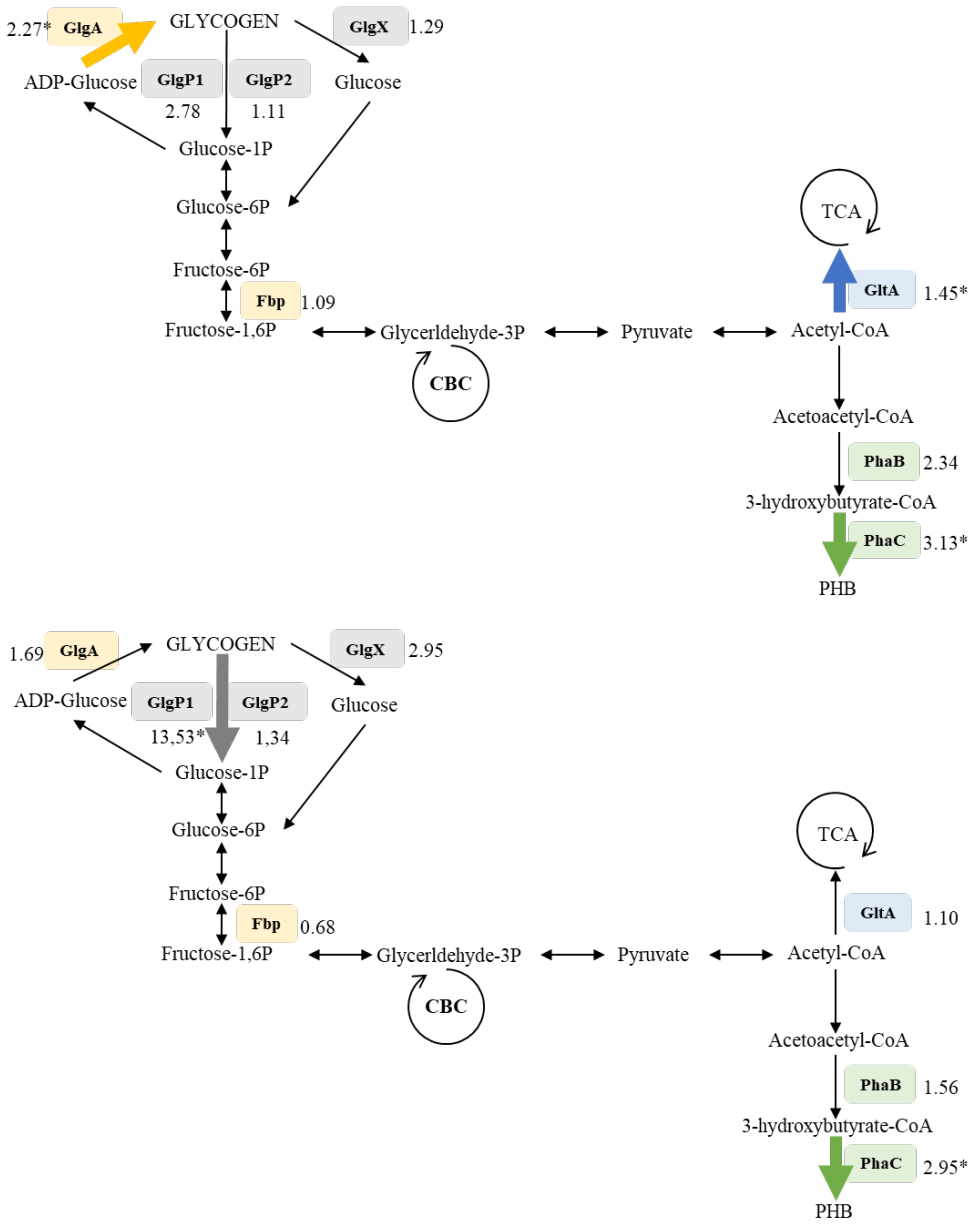

Figure 3. Schematic representation of biosynthetic pathways for PHB and glycogen production in cyanobacteria. (A) corresponds to results from day 105 and (B) day 108. Enzymes codified by the studied genes are shown in squares. Numbers next to enzymes names represent the fold gene expression. * denotes genes with statistically significant overexpression (p-value < 0.05). Yellow shows key enzymes involved in the synthesis of glycogen (Fbp, GlgA); grey, to the glycogen catabolism (GlgP1, GlgP2, GlgX); green, to the synthesis of PHB (PhaB, PhaC); and blue, to the introduction of acetyl-CoA into the tricarboxylic acid (TCA) cycle (GltA). Abbreviations: Fbp: fructose-bisphosphatase 1 GlgA: glycogen synthase, GlgP1 and glgP2: glycogen phosphorylase, GlgX: glycogen

debranching enzyme, GltA: citrate synthase, PhaB: Acetyl-CoA reductase, PhaC: poly(3-hydroxyalkanoate) synthase, TCA: tricarboxylic acid cycle, CBC: Calvin-Benson cycle.

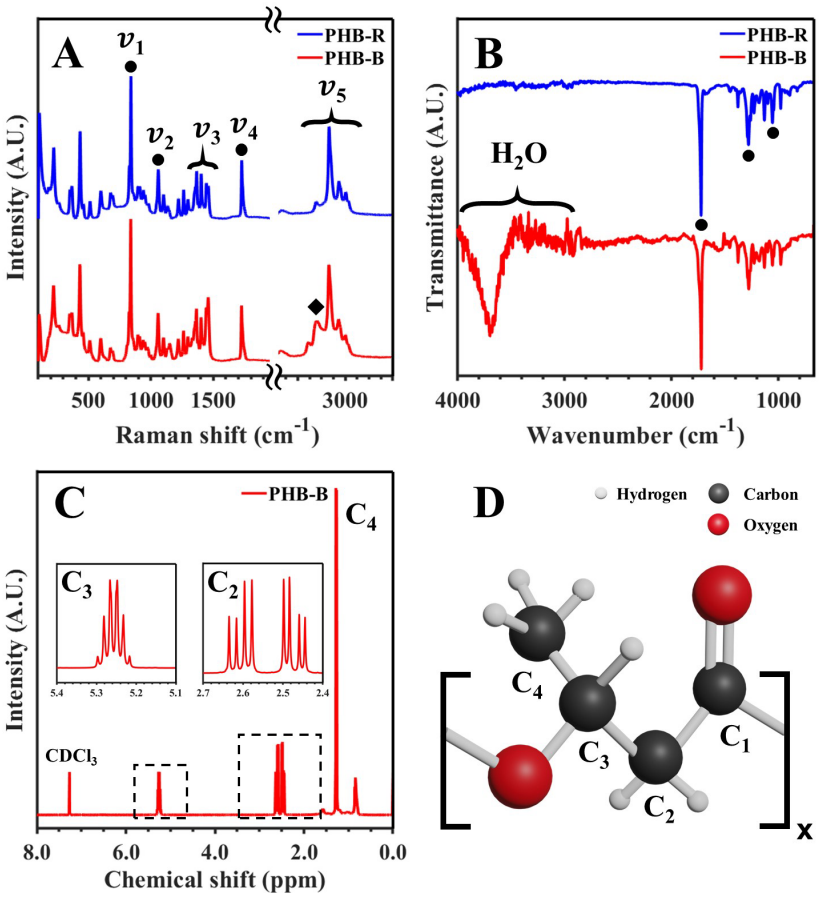

Figure 4. (A) Raman spectra for the PHB-R and PHB-B samples where the main Raman active modes are marked with circles. The diamond highlights the shoulder attributed to impurities during the extraction process. (B) FTIR spectra for the samples PHB-R and PHB-B, where the region affected by the water and the vibrational modes (marked with circles) can be observed. (C) ^{1}H-NMR spectra for the PHB-B sample with insets of the relevant peaks and carbon assignation related to the monomer carbons. (D) Schematic drawing of the PHB monomer with carbon numeration for NMR spectra interpretation.